

# Lab on a Chip

Accepted Manuscript



This is an *Accepted Manuscript*, which has been through the Royal Society of Chemistry peer review process and has been accepted for publication.

*Accepted Manuscripts* are published online shortly after acceptance, before technical editing, formatting and proof reading. Using this free service, authors can make their results available to the community, in citable form, before we publish the edited article. We will replace this *Accepted Manuscript* with the edited and formatted *Advance Article* as soon as it is available.

You can find more information about *Accepted Manuscripts* in the [Information for Authors](#).

Please note that technical editing may introduce minor changes to the text and/or graphics, which may alter content. The journal's standard [Terms & Conditions](#) and the [Ethical guidelines](#) still apply. In no event shall the Royal Society of Chemistry be held responsible for any errors or omissions in this *Accepted Manuscript* or any consequences arising from the use of any information it contains.

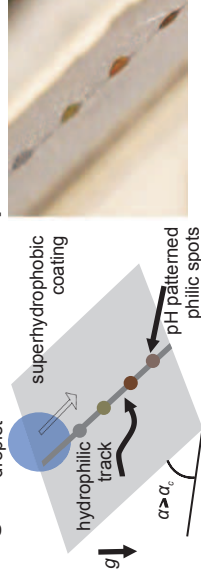


**Table of Contents Graphic Caption**

Inkjet-patterned hydrophilic spots on superhydrophobic paper overlaid with pH indicators to create a point-of-care diagnostic device for droplet sampling at 50 Hz.

# Inkjet patterned superhydrophobic paper for open-air surface microfluidic devices<sup>§</sup>

Mohamed Elsharkawy<sup>a</sup>Thomas M. Schutzius<sup>a</sup>Constantine M. Megaridis<sup>\*a</sup>

## Abstract

We present a facile approach for the fabrication of low-cost surface biomicrofluidic devices on superhydrophobic paper created by drop-casting a fluoroacrylic copolymer onto microtextured paper. Wettability patterning is performed with a common household printer, which produces regions of varying wettability by simply controlling the intensity of ink deposited over prespecified domains. The procedure produces surfaces that are capable of selective droplet sliding and adhesion, when inclined. Using this methodology, we demonstrate the ability to tune the sliding angles of 10  $\mu\text{L}$  water droplets in the range from 13° to 40° by printing lines of constant ink intensity and varied width from 0.1 mm to 2 mm. We also formulate a simple model to predict the onset of droplet sliding on printed lines of known width and wettability. Experiments demonstrate open-air surface microfluidic devices that are capable of pumpless transport, mixing and rapid droplet sampling ( $\sim 0.6\mu\text{L}$  at 50Hz). Lastly, post treatment of printed areas with pH indicator solutions exemplifies the utility of these substrates in point-of-care diagnostics, which are needed at geographical locations where access to sophisticated testing equipment is limited or non-existent.

<sup>§</sup>Electronic Supplementary Information (ESI) available: Mathematical derivation, accompanying images, and videos are available in the supplementary information. See DOI:

<sup>a</sup>Department of Mechanical and Industrial Engineering, University of Illinois at Chicago, Chicago, IL 60607, USA. Fax: (312) 413-0447; Tel: (312) 996-3436; E-mail: cmm@uic.edu

## 1 Introduction

Surfaces with water droplet contact angles exceeding  $150^\circ$  and sliding angles below  $10^\circ$  are deemed superhydrophobic and self-cleaning. It has been shown that surfaces demonstrating superhydrophobicity, whether natural or artificial, can be modified to yield domains of varying wettability (e.g., superhydrophobic-hydrophilic). Methods of such modification include, but are not limited to plasma,<sup>2</sup> chemical,<sup>3</sup> and photo-lithographic treatment.<sup>4</sup> In recent years, this superhydrophobic-hydrophilic behavior has formed the basis for producing surface microfluidic devices. Arrangements with patterned wettability have been studied in pool boiling,<sup>5</sup> fog capture,<sup>3</sup> selective droplet control, droplet splitting, among other applications. Being able to produce microfluidic devices that combine several of these behaviors into a single system, while at the same time maintaining a low-cost of production and easy assembly has implications in the areas of point-of-care (POC) and lab-on-chip analytical devices. One of the steps in producing low-cost surface-microfluidic devices is choosing an appropriate substrate for patterning. Due to its low cost, flexibility, versatility, light weight, and abundance, paper is already the basis of several household POC diagnostic devices (e.g., pregnancy tests, strips for urinalysis, litmus strips, etc.) Over the past several decades, such diagnostic devices have helped spawn a \$2.1 billion market that spans over 200 companies and has far reaching implications in the clinical, environmental, and bio-defense industries.<sup>6</sup>

Paper-based, disposable POC devices hold high hopes for utilization in economically developing environments.<sup>7</sup> For these devices to be effective and mass applicable, they must be able to store, transport, split, and analyze droplets of a given size and liquid, while simultaneously being low-cost and easy-to-produce with minimal resources; such properties are not inherent to paper materials. In order to produce these desired behaviors, one must develop the ability to selectively pattern varying wettability on paper substrates with the spatial resolution required for each application.

Several techniques have already been reported for the production of surface microfluidic devices on various substrates. Xing et al.<sup>8</sup> reported hydrophobic surfaces that were laser-patterned to produce superhydrophobic channels, which were then primed with water, before droplets were added at the end of the aforementioned channels, eventually coalescing into one another. One method to induce a passive pumping mechanism has mimicked the natural behavior of the cribellate spider *Uloborus walckenaerius*.<sup>9</sup> Watanabe<sup>10,11</sup> fabricated “surface-directed channels” with superhydrophobic glass substrates (PDMS-coated) that were inkjet patterned with a specially designed solution composed of 2-(2-ethoxyethoxy) ethanol and assembled to produce channels that

relied on capillary action to induce droplet mobility and wetting. Abe et al.<sup>12</sup> demonstrated significant advancement in the field by developing filter paper substrates selectively patterned via inkjet printing for multianalyte and immuno-chemical sensing. The combination of commercially available paper, printers, and ink used to induce varying areas of wettability has been reported by Balu et al.,<sup>13</sup> Barona and Amirfazli<sup>14</sup> and Sousa and Mano.<sup>15</sup> Balu et al.<sup>13</sup> utilized previously reported model paper substrates that were plasma-treated to induce superhydrophobicity and were then patterned using common printer ink to produce "sticky islands." These islands were analyzed and implemented for droplet storage, transferring, mixing and splitting. Barona and Amirfazli<sup>14</sup> presented a sprayable superhydrophobic nanocomposite film that was patterned via inkjet printing with varying "intensities" of ink. These surfaces were then tested for water repellency and droplet mobility. Sousa and Mano<sup>15</sup> produced superhydrophobic paper which was patterned by inkjet printing and writing. The same type of paper was also modified by poly-(hydroxybutrate) and protein absorbers in demonstrating the viability of such substrates as disposable lab-ware and lab-on-paper devices.<sup>16</sup> Finally, Li et al.<sup>17</sup> combined plasma etching and sandpaper to induce controlled droplet splitting on superhydrophobic paper. Noting these previous works, we have developed a cost-effective, comprehensive system that not only mimics the aforementioned behaviors on a single substrate, but also demonstrates potential for further applications in droplet sampling, testing, controlling lab-on-paper reactions, and selectively mobilizing small liquid volumes.

In this paper, we set out to produce low-cost surface microfluidic devices via inkjet printing onto microtextured silicon carbide paper (sandpaper) that was coated with a fluoroacrylic copolymer to yield a superhydrophobic baseline surface. The sandpaper is used as an example of a myriad of papers that are available in the open market. The surface microfluidic devices, in combination with the underlying paper substrate, function as a viable platform for paper-based POC diagnostic devices designed on the principles of patterned wettability. The end result is a versatile surface capable of performing a variety of tasks ranging from droplet mixing and sampling, selective droplet mobility, and pumpless surface microfluidics, culminating in the creation of a simple paper-based POC device. Previous papers have reported the design of inkjet based processes, paper microfluidic devices, and POC devices; we build on these previous works and create an easy-to-use, easy-to-produce versatile system capable of demonstrating the aforementioned properties. Paper's versatility and flexibility make it an ideal surface to be used in combination with common inkjetting techniques. Inkjetting as a patterning technique has gained momentum over the past few years due

to its ability to accurately deposit picoliter volume liquids over a range of variant substrates. With their low cost of operation, abundance, ease of use, and good patterning accuracy, paper substrates present themselves as a powerful alternative for modern photolithographic<sup>4</sup> and laser patterning techniques.<sup>18</sup>

## 2 Experimental

### 2.1 Materials

Silicon carbide paper sanding sheets (1500 grit;  $\sim 10\mu\text{m}$  feature size; McMaster-Carr) were used. An over-the-counter inkjet printer (Kodak Office Hero 1.609) and ink (Kodak black and color ink cartridges, 10 series) were obtained locally. The chemicals utilized are aqueous fluoroacrylic copolymer dispersion (PMC, 20 wt.% in water, Capstone<sup>®</sup> ST-100, DuPont), acetic acid (99.9 wt.%, Fisher Scientific), acetone (ACS reagent,  $\geq 99.5\%$ ; Sigma-Aldrich), alizarin yellow (ACS reagent, dye content 50%; Sigma Aldrich), bromothymol blue (ACS reagent, dye content 95%; Sigma Aldrich), and methyl red (ACS reagent, dye content 95%; Sigma Aldrich).

### 2.2 Sample Preparation

To produce 10 g of hydrophobizing solution, 0.5 g of acetic acid, 0.5 g of PMC and 9.0 g of acetone were added in a vial. The solution was drop-casted onto the sandpaper and dried by a heat gun for 1 min (Proheat<sup>®</sup> Varitemp<sup>®</sup> PH-1200, 1300 W max). The coated sandpaper was then placed in an oven at 80°C for 60 min to dry completely.

### 2.3 Printing Process and Wettability Patterns

Advancing, receding and sliding angle measurements were performed on the uncoated (control) and coated sandpapers. Areas of varying ink intensity were then deposited on the coated substrates, which were fed through the inkjet printer. Ink deposition was controlled through the alteration of intensity in the printer's vector graphics editor. Within the software, the amount of ink deposited is controlled by a numbering system ranging from 0-100 (referred to as intensity); a 100 set value denotes 100 % intensity (*i.e.*, highest ink deposition rate). We note that the amount of deposited ink is correlated linearly with the intensity. For example, 100 % intensity corresponded to 0.5 g m<sup>-2</sup> ink add-on level, while 50 % intensity to 0.25 g m<sup>-2</sup>. At first, only black ink was deposited

onto the superhydrophobic paper surface in increments of 25 % (from 0-100) intensity. Afterwards, different colors were deposited at the same intensity increments in order to examine if there is differentiation between colors and the change of wettability they induce. After printing the desired ink patterns on the aforementioned superhydrophobic sandpaper, the printed paper was once again dried with the heat gun and left to dry in the oven (80°C) for an additional 60 minutes. This protocol assured complete ink drying. If ink had not dried properly, ink dissolution occurred when coming in contact with water. Once the printed areas were thoroughly dried, sliding, receding and advancing contact angle measurements for water were performed. Based on the obtained results, smaller increments of intensity (5 %) were printed in order to hone on intensities that correlate to transitional values (*e.g.*, hydrophobic-hydrophilic, sliding-immobile). The results are discussed in the following section. Next, tracks of varying width were printed with a constant cyan ink intensity, although other primary colors behaved similarly. Using different combinations of track width and ink intensity, a system was designed where droplet sliding could be selectively controlled (in terms of the inclination angle,  $\alpha$ ). In order to demonstrate the versatility of the produced substrates, different patterns were printed for different microfluidic functions. One pattern demonstrated Laplace-pressure-driven motion, while printed tracks demonstrated water droplet sliding control. In addition, a spot sampling pattern was used to demonstrate rapid droplet splitting and sampling.

### 3 Results and Discussion

In order to develop a biomicrofluidic system based upon tuning droplet mobility, it is first necessary to synthesize superhydrophobic surfaces. It is well established that the two main factors that govern the liquid repellency of a given surface are its chemical nature (surface energy) and topographical microstructure (surface roughness). In general, a substrate is incapable of achieving a superhydrophobic state without a certain extent of underlying roughness and chemical hydrophobicity. Thus, modern techniques utilized in creating superhydrophobic substrates rely on manipulating both the roughness and surface energy of the substrate. Sandpaper already possesses the necessary underlying roughness, thus requiring only manipulation of its surface energy to attain superhydrophobicity. Scanning electron microscopy (SEM) images of the substrates were taken before and after coating with PMC. **Figure 1** presents micrographs of the SiC micro-textured substrate after coating with PMC and shows that it forms a conformal film (roughness features of 10  $\mu\text{m}$ ), which

is advantageous for generating superhydrophobic surfaces.

The required PMC solution concentration for superhydrophobizing the sandpaper was estimated by intending to form a thin, conformal film around the pre-existing silicon-carbide microtexture (feature sizes about  $10\ \mu\text{m}$ ). Acetone readily spread on the silicon-carbide micro-textured surface to form a  $\sim 100\ \mu\text{m}$  thick film. Therefore, when a 1 wt.% PMC solution in acetone was deposited onto the micro-textured substrate, after it dried, PMC was estimated to form a  $\sim 1\ \mu\text{m}$  film, which is on the scale or below the smallest primary surface feature size, thus ensuring that a large amount of texture remains exposed, as supported by the SEM images in Figure 1. Prior to coating, the sandpaper had advancing contact angle of approximately  $106^\circ \pm 4.8^\circ$  and receding contact angle of  $\approx 0^\circ$ , implying that the uncoated sandpaper already lies in the hydrophobic (but immobile liquid) regime. Coating by PMC resulted in an advancing contact angle of  $156^\circ \pm 4.5^\circ$  and receding angle of  $130^\circ \pm 6.3^\circ$ , with sliding angle of  $13^\circ \pm 2.4^\circ$ . This transition into the superhydrophobic regime can be attributed to the pre-existing roughness of the sandpaper and the hydrophobic nature of the overlaying PMC film.

Next, black ink was deposited on the superhydrophobic paper via inkjet printing. Deposition of the ink was controlled by prescribing ink intensity in the printer's drawing software. An SEM image of black ink deposited at 100 % intensity on the superhydrophobic (coated) sandpaper is presented in Figure 2. The excessive amount of ink deposited alters the surface energy of the substrate, thus changing its inherent wettability. Subsequently, black ink intensity was altered in increments of 25; advancing and receding angle measurements were performed and are summarized in Figure 3. For the maximum deposition of black ink (100 %), we recorded an advancing angle of  $96^\circ \pm 5.4^\circ$ ; the receding angle was practically zero; therefore, the droplets did not display sliding behavior. This sharp decline in liquid repellency and mobility signifies the shift of the superhydrophobic paper state into the hydrophobic, borderline, hydrophilic regime. This change can be attributed to the increase of surface energy of the substrate due to the presence of the ink. As shown in Figure 2, the ink on the coated substrate forms a layer which the overlaying droplet encounters. The presence of the ink lowers liquid mobility, and, in turn, the repellent property of the substrate. By varying the amount of ink deposited, one can modify the degree by which the surface energy of the substrate is altered. In addition, an excessive amount of ink can, theoretically, reduce the amount of surface roughness. Thus, by varying the intensity (*e.g.*, amount) of the applied black ink, one can selectively control droplet mobility and repellency, as previously reported by Barona

and Amirfazli.<sup>14</sup> Repeating the same experiments with cyan, magenta and yellow inks separately, we noted a similar behavior.

Black ink was inkjetted next using deposition intensity increments of 5, from 25 to 50 (0.125 to 0.25 g m<sup>-2</sup>). The upper bound of this range was selected as the point of transition for droplet sliding (**Figure 4**). The hypothesis was that this enhanced scale of ink deposition would allow the selective tuning of droplet mobility, as based on the amount of ink deposited. As shown in **Figure 4**, the sliding angle continued to increase as the amount of ink gradually increased, thus demonstrating the ability to control droplet sliding angle by specifying the amount of ink deposited on the substrate. This process presents a "chemical" approach to control droplet mobility on a textured solid. The results indicate that prescribed amounts of ink can effectively alter the surface energy of the substrate, while leaving the underlying microtexture largely unaffected (**Figure 2**).

The above approach demonstrated control of liquid mobility by way of changing the surface energy of the substrate. We now demonstrate another method for droplet sliding control via contact-area manipulation (**Figure 5**). Linear tracks of varying width ranging from 0.1 mm to 2 mm were printed with cyan ink at 47 % intensity and tested with 10 μL water droplets. The sliding angle results are presented in **Table 1**. As track width increases, so does the droplet sliding angle. This decrease in mobility is a result of increased contact line distortion between the track width and the receding line.<sup>19</sup> Thus, by simply varying the width of the printed lines, we can control the sliding angle of the droplets placed on the substrate (demonstration presented in ESI<sup>4</sup> Section 2.1). Such a mechanism can be beneficial in systems that require controlled droplet release. Applying Extrand and Gent's<sup>1</sup> analysis of retention of liquid droplets, we can model the ability of the present surfaces to control sliding angle. The retentive force  $F_R$  of a spherical droplet on a solid surface is given by

$$F_R = F_r - F_a \quad (1)$$

where  $F_r$  is the force from the rear of the droplet and  $F_a$  from the advancing droplet front. Following Extrand and Gent's<sup>1</sup> derivation,

$$F_a = 2R\gamma \cos \theta_a \quad (2)$$

and

$$F_r = 2 \int_0^{\pi/2} R\gamma \cos \theta \cos \phi d\phi \quad (3)$$

where  $R$  is the droplet radius,  $\gamma$  the surface tension of the liquid,  $\phi$  (see ESI<sup>4</sup> **Figure S1**) the azimuthal angle that circumnavigates the droplet contact line from the rearmost point ( $\phi=0$ ) to the side of the drop ( $\phi=\pi/2$ ); due to the geometry, we need to consider only values up to  $\phi=\pi/2$ . Following Extrand and Gent,  $\cos \theta$  varied linearly around the perimeter between the receding value  $\cos \theta_r$  at the rear of the drop ( $\phi=0$ ) and the advancing value  $\cos \theta_a$  at the side of the drop ( $\phi=\pi/2$ )

$$\cos \theta = \frac{\phi}{\pi/2} \cos \theta_a + \left(1 - \frac{\phi}{\pi/2}\right) \cos \theta_r \quad (4)$$

In the present situation where the droplet slides on the wettable path and extends outward over the phobic domain, the liquid does not encounter a homogeneous contact surface. Thus, the  $\cos \theta_a$  and  $\cos \theta_r$  terms vary according to the surface properties underneath the droplet. In order to accommodate for this spatial inhomogeneity, **Equations (2), (3), and (4)** are modified accordingly. In particular, the integral defined in Equation (3) is replaced by the sum of two separate integrals, each corresponding to a different surface under the liquid volume

$$F_r = F_{r_1} + F_{r_2} = 2R\gamma \int_0^{\phi_1} \cos \theta_1 \cos \phi d\phi + 2R\gamma \int_{\phi_1}^{\pi/2} \cos \theta_2 \cos \phi d\phi \quad (5)$$

where  $F_{r_1}$  is the rear force contribution by the philic track,  $F_{r_2}$  the rear force contribution by the phobic paper,  $\phi_1 = \sin^{-1} \left(\frac{w}{2R}\right)$  (see ESI<sup>4</sup> **Figure S1**) the value of  $\phi$  at the contact line point separating the philic track from the phobic domain,  $w$  the width of the track, and  $\cos \theta_i$  are modified forms of equation (4); see ESI<sup>4</sup> Section 1. In order to calculate the total retentive force,  $F_R$ , an analogous analysis for the advancing force is followed

$$F_a = F_{a_1} + F_{a_2} = 2R\gamma \cos \theta_{a_{ink}} \int_0^{\phi_1} \cos \psi d\psi + 2R\gamma \cos \theta_{a_{paper}} \int_{\phi_1}^{\pi/2} \cos \psi d\psi \quad (6)$$

where  $\psi$  denotes the angle from the front end of the droplet. In line with Extrand and Gent's derivation,<sup>1</sup> we assumed that the advancing angle is constant for each of the two surfaces (paper or ink-coated track) which the liquid encounters. Combining **Equations (5) and (6)** into **Equation (1)** we determine  $F_R$ , which is equated with the gravity force on the droplet along the inclined surface, to obtain

$$F_R = mg \sin \alpha_c \quad (7)$$

with  $m$  denoting the mass of the  $10\ \mu\text{L}$  droplet. This equation is used to estimate  $\alpha_c$ , the sliding angle at which the droplet starts moving down the slope. The predicted and experimental sliding angles are compared in **Table 1**. Nearly all predicted values are within one standard deviation of their experimentally-measured counterparts, supporting the argument that droplet sliding is controlled only by wettability forces.

To demonstrate a POC-type device, a linear repeated spot pattern was printed as shown in **Figure 6a**. The circular reservoirs (1.5 mm diameter) were printed with 100 % black ink, while the connecting line (0.1 mm wide) was printed with 35 % cyan ink. The four printed black spots functioned as sticky islands, while the line track acted as a guiding rail for a droplet released down the inclined ( $20^\circ$ ) plane. The hydrophilic spots were post processed with the water-soluble pH indicators mentioned in the materials section. By placing a  $10\ \mu\text{L}$  droplet at the top of the tilted pattern, the droplet rolled down, leaving behind a liquid sample on each of the sticky spots (for video see ESI<sup>4</sup> Section 2.2). This procedure successfully separated multiple small volumes (initially  $\sim 0.6\ \mu\text{L}$ ) from the original droplet at a rate of 50Hz. The maximum number of spot volumes that can be sampled from a single droplet depends on the initial liquid volume. The spot samples could be automatically analyzed by the pH indicators present on each spot. Due to the fact that each of the indicators reacts at different pH levels, a neutral droplet of water (pH=7) is expected to induce different color changes in each of the spotted regions; see **Figure 6b**. This functionality has potential for use in POC devices. For example, post-processing the philic spots with protein sensors, bacterial indicators or chemical reagents facilitates analytic procedures from a single droplet that is rapidly split as shown in **Figure 6**. The use of inkjet printing as a patterning technique, and the rapid droplet sampling procedure demonstrated herein in conjunction with post-processing methods, help lay forth the groundwork. Such simple but reliable droplet analysis procedures are necessary, especially in environments and conditions where supplies are scarce and testing facilities possess limited capabilities.

We now exploit the flexibility of the patterning technique in the design and implementation of surface microfluidic devices capable of capillary-driven fluidic transport and spontaneous droplet splitting. A dumbbell shaped flat pattern (**Figure 7**), similar to that examined by Xing et al.,<sup>8</sup> was printed (100 % black ink) onto the superhydrophobic paper substrate, which was kept horizontal. The pattern consisted of two circular reservoirs, 4 mm and 2 mm diameters, connected with a 25 mm long track of fixed width of 0.75 mm. Droplets of  $10\ \mu\text{L}$  and  $7\ \mu\text{L}$  were deposited on the

reservoirs (large and small, respectively) and the connecting channel was primed by adding water until a thin film formed. The pressure difference in the two volumes drove a flow from the smaller radius reservoir to the larger one, as seen in **Figure 8**. As Xing et al.<sup>8</sup> described, the flow rate is controlled by several factors, such as reservoir radii, channel width, and channel length. Using the present patterning approach, the above-mentioned factors can be controlled with precision by way of the vector graphics software of the inkjet printer, with minimal wait time. Thus, the present method offers an ideal mechanism for controlled mixing of different liquids on paper.

Due to the ease and flexibility of the patterning process, any imaginable 2D device can be printed. An example of one possible functional surface can be a repeated triangular pattern that functions as an energy barrier and induces anisotropic droplet sliding. Similar devices have already proven viable when produced on different surfaces.<sup>20</sup> Furthermore, if the previously described printed lines were positioned horizontally, and the width and ink deposition were tuned as needed, one could selectively control liquid adherence to the surface simply based on droplet size. Thus, the present approach offers a viable alternative to a recently reported method<sup>21</sup> that created invisible gates to moving water droplets by superhydrophobic metal-polymer hybrid surfaces featuring wettability gradients.

## 4 Conclusion

We presented a low-cost, facile method to produce superhydrophobic paper by coating common sandpaper with a commercially available fluoroacrylic copolymer (PMC). The underlying roughness of the sandpaper combined with the natural hydrophobic state of PMC resulted in advancing, receding, and sliding angles of  $156^\circ \pm 4.5^\circ$ ,  $130^\circ \pm 6.3^\circ$ , and  $13^\circ \pm 2.4^\circ$ , respectively. The superhydrophobic substrates were patterned with a common household inkjet printer to produce wettable domains. Varying intensities of black ink (up to  $0.5 \text{ g m}^{-2}$  add-on rate) were patterned onto the substrates, which were dried and tested for water droplet wettability and mobility. As the amount of ink deposited increased, the wettability of the surface improved and the droplet mobility decreased (surface became sticky). There was little to no quantitative difference in modifying wettability among the different ink colors. At 50 % ink deposition ( $0.25 \text{ g m}^{-2}$ ), droplet mobility was entirely impeded for all ink colors. Line tracks with 50 mm length and width varying from 0.1 mm to 2 mm were created by depositing 47 % cyan ink. Using the aforementioned lines, the tests revealed good control and tuning of droplet sliding from mobile (0.1 mm track) to immobile (2 mm track).

A theoretical model accurately predicted the droplet release inclination angle for printed lines of known width and wettability. Specially printed areas exemplified the construction of low-cost microfluidic devices capable of splitting, storing, and analyzing water droplets of a given size. The present technique holds promise for expanding the utility of superhydrophobic paper substrates into the regime of point-of-care diagnostics.

## 5 Acknowledgments

This material is based upon work supported by the National Science Foundation Graduate Research Fellowship under Grant No.0907994. The authors would like to thank Dr. Ranjan Ganguly for his valued input in regards to the droplet sliding analysis.

## References

- [1] C. Extrand and A. Gent, *Journal of Colloid and Interface Science*, 1990, **138**, 431–442.
- [2] D. Teare, C. Spanos, P. Ridley, E. Kinmond, V. Roucoules, J. Badyal, S. Brewer, S. Coulson and C. Willis, *Chemistry of Materials*, 2002, **14**, 4566–4571.
- [3] L. Zhai, M. C. Berg, F. . Cebeci, Y. Kim, J. M. Milwid, M. F. Rubner and R. E. Cohen, *Nano Letters*, 2006, **6**, 1213–1217.
- [4] A. Martinez, S. Phillips, M. Butte and G. Whitesides, *Angewandte Chemie International Edition*, 2007, **46**, 1318–1320.
- [5] A. R. Betz, J. Xu, H. Qiu and D. Attinger, *Applied Physics Letters*, 2010, **97**, 141909.
- [6] G. E. Fridley, C. A. Holstein, S. B. Oza and P. Yager, *MRS Bulletin*, 2013, **38**, 326–330.
- [7] C. Sicard and J. D. Brennan, *MRS Bulletin*, 2013, **38**, 331–334.
- [8] S. Xing, R. S. Harake and T. Pan, *Lab on a Chip*, 2011, **11**, 3642–3648.
- [9] Y. Zheng, H. Bai, Z. Huang, X. Tian, F.-Q. Nie, Y. Zhao, J. Zhai and L. Jiang, *Nature*, 2010, **463**, 640–643.
- [10] M. Watanabe, *Lab on a Chip*, 2009, **9**, 1143–1146.
- [11] M. Watanabe, *Microfluidics and Nanofluidics*, 2010, **8**, 403–408.

- [12] K. Abe, K. Suzuki and D. Citterio, *Analytical Chemistry*, 2008, **80**, 6928–6934.
- [13] B. Balu, A. D. Berry, D. W. Hess and V. Breedveld, *Lab on a Chip*, 2009, **9**, 3066–3075.
- [14] D. Barona and A. Amirfazli, *Lab on a Chip*, 2011, **11**, 936–940.
- [15] M. Sousa and J. Mano, *Cellulose*, 2013, **20**, 2185–2190.
- [16] M. P. Sousa and J. F. Mano, *ACS Applied Materials & Interfaces*, 2013, **5**, 3731–3737.
- [17] L. Li, V. Breedveld and D. W. Hess, *Colloid and Polymer Science*, 2013, **291**, 417–426.
- [18] T. M. Schutzius, I. S. Bayer, G. M. Jursich, A. Das and C. M. Megaridis, *Nanoscale*, 2012, **4**, 5378–5385.
- [19] T. Furuta, M. Sakai, T. Isobe, S. Matsushita and A. Nakajima, *Langmuir*, 2011, **27**, 7307–7313.
- [20] A. Nakajima, Y. Nakagawa, T. Furuta, M. Sakai, T. Isobe and S. Matsushita, *Langmuir*, 2013, **29**, 9269–9275.
- [21] D. Ishii and M. Shimomura, *Chemistry of Materials*, 2013, **25**, 509–513.

## 6 Figures

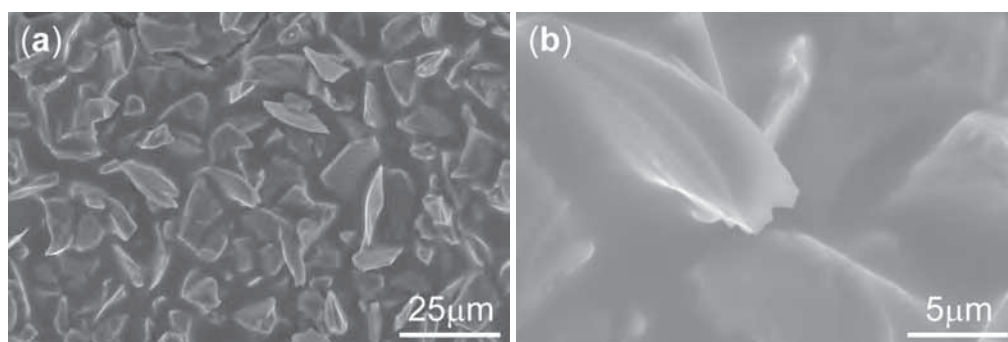


Figure 1: (a) SEM image of 1500 grit sandpaper coated with a fluoropolymer film (PMC). The sandpaper already possesses the necessary underlying surface roughness required to bring about a superhydrophobic state. (b) Magnified detail of a micro-feature spot on (a).

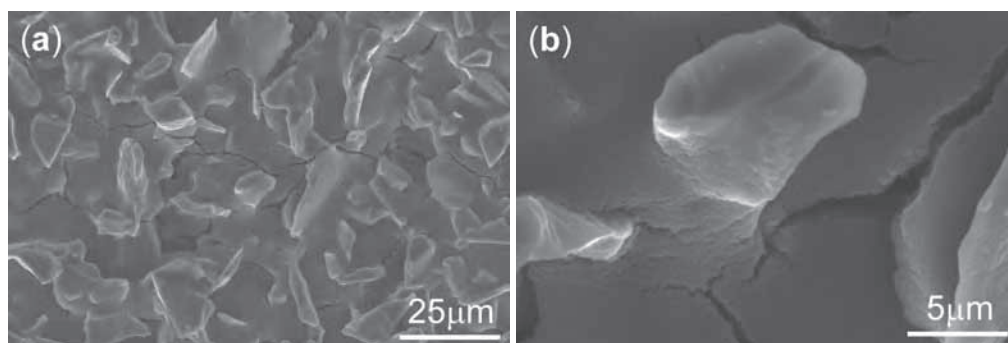


Figure 2: SEM images of superhydrophobic paper covered with black ink dispensed by an inkjet office printer. Magnification increases from (a) to (b). The deposited ink alters the underlying surface energy of the surface. This, in effect, changes the wettability of the substrate. By selectively increasing or decreasing the amount of ink deposited, one can modulate the wettability, as desired.

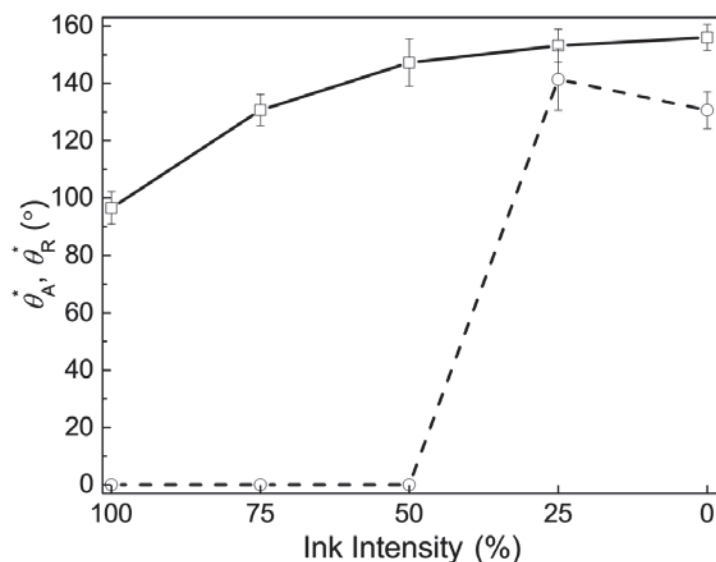


Figure 3: Advancing (squares; solid line) and receding (circles; dashed line) water contact angle measurements on sandpaper printed with different amount of black ink. The amount of deposited ink correlated linearly with the intensity value (100 % corresponded to  $0.5 \text{ g m}^{-2}$  ink add-on level; 50 % to  $0.25 \text{ g m}^{-2}$ ). As the amount of ink deposited increased, so did the wettability. This is due in part to the increased surface energy provided by the ink, and the partial smoothing of the underlying texture by the formation of the ink layer on the substrate's rough terrain. Furthermore, the steep decrease of receding contact angle between 25 % and 50 % intensity makes possible the manipulation of the sliding angle.

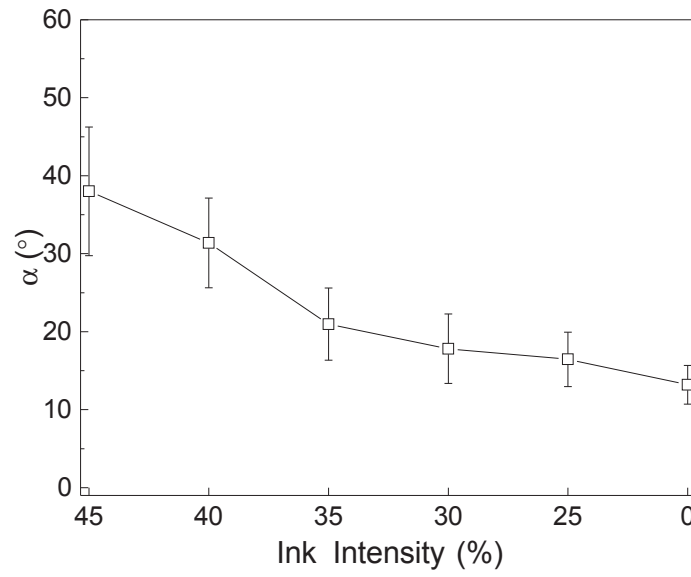


Figure 4: Water droplet sliding angle ( $\alpha$ ) vs. black ink intensity in increments of 5 % from 25 % to 45 %. As the intensity rose, so did the sliding angle. For intensities equal or greater than 50 %, the droplets remained immobile. These phenomena are supported and understood by the advancing-receding contact angle data in Figure 3.

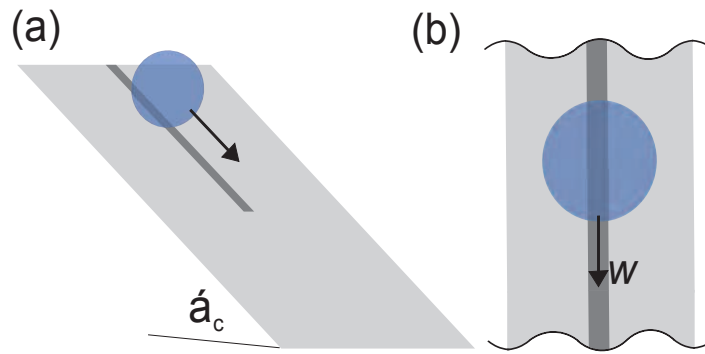


Figure 5: (a) Water droplet placed onto a hydrophilic line track of a known (but varied) width  $w$ ; the track was inkjet printed on superhydrophobic paper (light grey). The droplet started sliding down the track when the paper tilt angle reached a threshold value  $\alpha_c$  that correlated with the track width  $w$ . (b) Top view.

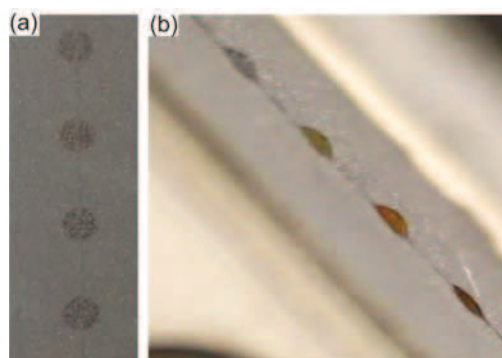


Figure 6: (a) Black ink deposited on superhydrophobic paper at 100 % intensity ( $0.5 \text{ g m}^{-2}$ ) to form hydrophilic 1.5 mm dia. spots connected by a 0.1 mm wide line serving as rail for a droplet rolling down the inclined plane. Each circular region was patterned with a separate water soluble pH indicator: alizarine yellow, bromothymol blue, or methyl red. The first (top most) spot was untreated, and thus acted as a control for color. (b) The substrate was angled at  $20^\circ$  and a  $10 \mu\text{L}$  water droplet was placed at the top. Due to the superhydrophobic nature of the substrate and its low sliding angle, the droplet slid and rolled over the hydrophilic spots at a rate of 50 spots per second. After making contact with each spot, the droplet released a small volume ( $\sim 0.6 \mu\text{L}$ ) and continued on to the next spot. The liquid left behind on each spot interacted with the pre-deposited pH indicator, and thus changed color accordingly.



Figure 7: Black (100 % intensity), hydrophilic pattern inkjetted on microtextured, silicon-carbide, superhydrophobic paper. The top (large) spot reservoir is 4 mm in diameter and the bottom (small) reservoir is 2 mm in diameter. The connecting line track is 25 mm long and 0.75 mm wide.

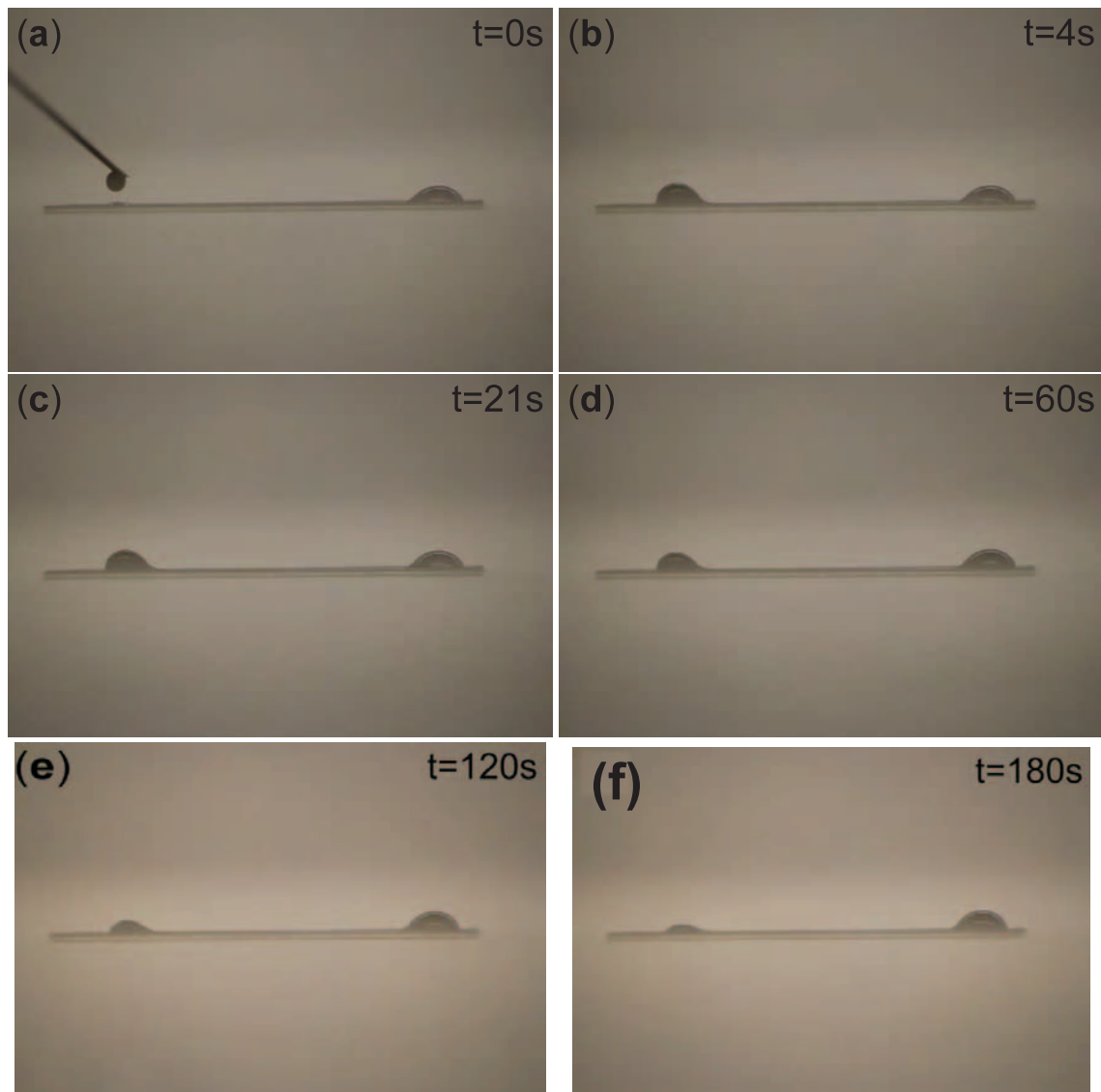


Figure 8: (a)  $7\ \mu\text{L}$  water droplet being placed with a syringe and 25 gauge needle onto the 2mm-dia. reservoir shown in Figure 7 (top view). The larger 4mm reservoir (right) contains a pre-deposited  $10\ \mu\text{L}$  droplet; (b)-(e) time sequence of images showing the gradual draining of the small droplet (left) into the large droplet (right). The flow is driven by the Laplace pressure difference between the two droplets.<sup>8</sup>

## 7 Tables

Line width $w$ (mm)	Predicted $\alpha_c$ from Eq. (7)	Measured $\alpha_c$
0.0	11.3°	13.2° ± 2.5°
0.1	21.1°	25.6° ± 3.8°
0.5	25.3°	28.7° ± 6.1°
1.0	30.8°	35.2° ± 5.7°
1.5	36.8°	36.5° ± 8.6°
2.0	43.7°	45.1° ± 4.0°

Table 1: Water droplet sliding angles on tracks of varying width printed with cyan ink at 47 % intensity. The sliding angle increased with line width, with the droplets losing mobility (*i.e.*, surface becomes sticky) above  $w = 2.0$  mm. Comparison of predicted angles with those measured experimentally.